RSC Advances

PAPER

View Article Online
View Journal | View Issue

Cite this: *RSC Adv.*, 2015, **5**, 32358

Synthesis and characterization of novel dumbbell shaped copolymers poly(ethylene oxide)$_x$-*b*-polystyrene-*b*-poly(ethylene oxide)$_x$ with tunable side arms by combination of efficient thiol-ene addition reaction with living polymerization mechanism

Lingdi Chen, Jian Huang, Xuepu Wang, Chengjiao Lu, Hongdong Zhang* and Guowei Wang*

Received 17th December 2014
Accepted 10th March 2015

DOI: 10.1039/c4ra16580b

www.rsc.org/advances

A series of novel dumbbell shaped copolymers poly(ethylene oxide)$_x$-*b*-polystyrene-*b*-poly(ethylene oxide)$_x$ (PEO$_x$-*b*-PS-*b*-PEO$_x$, x = 1, 2, 3) composed of different numbers of hydrophilic PEO and hydrophobic PS segments were prepared by combination of living anionic polymerization (LAP) and ring opening polymerization (ROP) mechanisms, and the efficient thiol-ene addition reaction was also adopted. First, the functional polystyrene with one hydroxyl group and one allyl group at each end (AGE-PS-AGE) was synthesized by the LAP of St monomers followed by the capping reaction with allyl glycidyl ether (AGE). Subsequently, by thiol-ene addition reaction with 2-mercaptoethanol (ME) and 3-mercapto-1,2-propanediol (MP), one allyl group on the AGE-PS-AGE was transformed into one or two hydroxyl groups to synthesize the functional polystyrene with two hydroxyl groups at both ends (ME-PS-ME) or three hydroxyl groups at both ends (MP-PS-MP). Then, the copolymers PEO$_x$-*b*-PS-*b*-PEO$_x$ were achieved by ROP of EO monomers using AGE-PS-AGE, ME-PS-ME and MP-PS-MP as macro-initiators. The target copolymers and their precursors were fully characterized by GPC, ^{1}H NMR and ^{13}C NMR measurements. The crystallization behavior of copolymers with different topologies and compositions was investigated by DSC, XRD and POM instruments, and the results showed that the topologies (compared to the compositions) tend to make the primary contribution to the crystallization behavior.

Introduction

In recent years, with the rapid development of living/controlled polymerization mechanisms and efficient coupling methods, a variety of polymers with complicated architectures and compositions have been realized by certain synthetic routes.[1] The unique architectures include graft,[2] hyper-branched,[3] cyclic,[4] dendritic,[5] star-shaped,[6] and so on,[7] and the compositions can be covered by plenty of segments derived from any polymerizable monomers. All these achievements can be attributed to the increasing interest on their unique physical properties in solution and bulk, as well as their versatile applications, including in biomedical materials,[8] nanotechnology,[9] composite materials[10] and supra-molecular science.[11]

Among all the compositions, polystyrene (PS) is a typical hydrophobic and amorphous segment, and poly(ethylene oxide) (PEO) is a hydrophilic and crystalline segment. Because of these characteristics, the copolymers containing both PS and PEO segments have been widely studied and utilized for various applications. For example, common models are the copolymers PS-*b*-PEO, PS-*b*-PEO-*b*-PS or PEO-*b*-PS-*b*-PEO with the simplest topologies. Research priorities for these copolymers have been focused on the microphase separated morphology,[12] thermodynamic properties,[13] crystallization behaviors,[14] and aggregate morphologies.[15] As for their applications, these copolymers can serve as template for porous materials[16] and micro/nano-patterns[17] based on their interesting self-assembly morphologies.[18] However, up to now, copolymers composed of PEO and PS segments with complicated architectures and defined molecular weights are still rarely researched, which might be attributed to the somewhat difficult synthesis procedure of these copolymers.

For copolymers with complicated architectures, a mere polymerization mechanism usually cannot reach the target.

State Key Laboratory of Molecular Engineering of Polymers, Collaborative Innovation Center of Polymers and Polymer Composite Materials, Department of Macromolecular Science, Fudan University, Shanghai 200433, China. E-mail: gwwang@fudan.edu.cn; Fax: +86 21 6564 0293; Tel: +86 21 6564 3049

Some efficient coupling reactions also play important roles in the synthesis of these copolymers. Until recently, innovative coupling reactions with "click" character include the thiol-bromide reaction,[19] thiol-ene addition reaction,[20] thiol-yne addition reaction,[21] Atom Transfer Radical Coupling (ATRC) reaction,[22] Glaser coupling,[23] Suzuki reaction,[24] Copper Catalyzed Azide/Alkyne Click (CuAAC) chemistry and Diels–Alder (DA) [4 + 2] reaction,[1f] and so on. Because of their high efficiencies and particular versatility, these reactions have been widely used in polymer chemistry. Among these coupling reactions, the thiol-ene addition reaction has been widely adopted because of its high efficiency and tolerance to water and functional groups, as well as its easy operation under photochemical initiation. Applications include nanotechnology,[25] composites,[26] biochemistry,[27] and adhesives.[28] Correspondingly, various monomers containing vinyl and thiol groups were designed and their thiol-ene addition reactions were well researched.[29] For example, Hawker,[30] Son[31] and Malmstrom[32] have synthesized several dendrimers *via* this versatile thiol-ene addition reaction. Hawker,[33] Kornfield,[34] Schlaad[35] and Sengupta[36] prepared several functionalized polymers (such as PS, poly(butadiene) (PB), and poly(propylene) (PP)) by using this technique under feasible and mild conditions, and telechelic polymers were also realized by Sumerlin[37] and Maynard.[38] Thus, this thiol-ene "click" chemistry has actually been proved to be an efficient, robust and orthogonal tool in polymer chemistry.

In this contribution, considering the above limitation on copolymers composed of PEO and PS segments with different architectures and defined molecular weights, we aim to synthesize some novel dumbbell shaped copolymers PEO_x-*b*-PS-*b*-PEO_x ($x = 1, 2, 3$) with tunable side arms (Scheme 1). The PS segment with controlled molecular weight could be realized by the typical living anionic polymerization (LAP) mechanism, and the PEO segment could be synthesized by the ring opening polymerization (ROP) mechanism. Also, thiol-ene "click" chemistry is adopted to modify the functionalized intermediate to tune the initiating sites (corresponding to the tunable arms of the target copolymers) on macro-initiators. On the other hand, in previous works, some researchers have studied the crystallization behavior of copolymers composed of PEO and PS segments.[39] These works were all focused on the effect of composition on their crystallization behavior, and the topologies were less considered.[40] Thus, in this contribution, as another important task, the crystallization behavior of the synthesized copolymers with similar compositions but different topologies are also investigated and compared.

Experimental

Materials

Styrene (St, 99%, Sinopharm Chemical Reagent Co. (SCR)) was washed with 10% NaOH aqueous solution followed by water three times successively, dried over anhydrous $MgSO_4$ for 24 h, further dried over CaH_2 and distilled under reduced pressure before use. Allyl glycidyl ether (AGE, Aldrich, 99%) was dried over CaH_2 and distilled under reduced pressure before use. Ethylene oxide (EO, SCR, 99%) was dried over CaH_2 and distilled before use. Naphthalene (SCR, AR) was purified by sublimation. Tetrahydrofuran (THF, SCR, 99%) was refluxed and distilled from potassium naphthalenide solution. Azobisisobutyronitrile (AIBN, SCR, 99%), *n*-butyllithium (*n*-BuLi, 1.6 M solution in hexane, J&K), 2-mercaptoethanol (ME, Aldrich, 98%) and 3-mercapto-1,2-propanediol (MP, Aldrich, 98%) were used as received. Diphenylmethyl potassium (DPMK) with a concentration of 0.75 mol L^{-1} was prepared as described

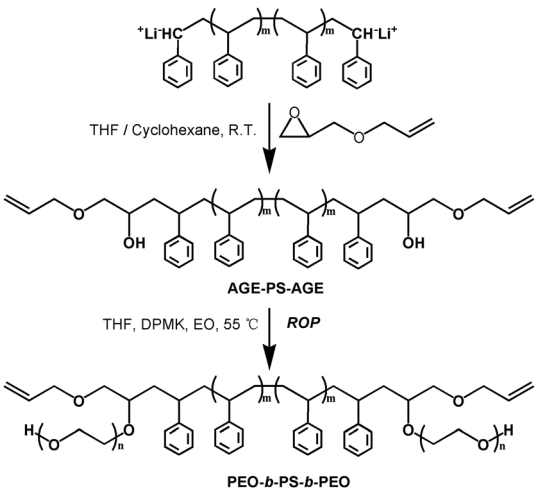

Scheme 2 The synthetic procedure of copolymers PEO-*b*-PS-*b*-PEO and their precursor.

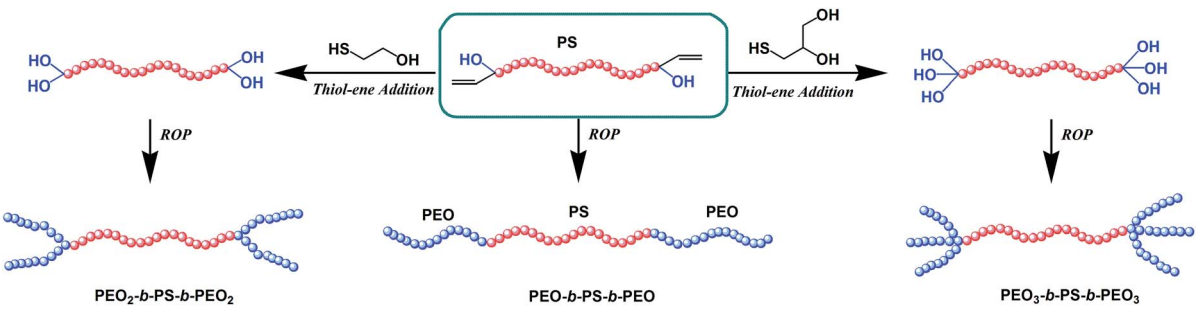

Scheme 1 The illustration of synthetic procedure of copolymers PEO_x-*b*-PS-*b*-PEO_x.

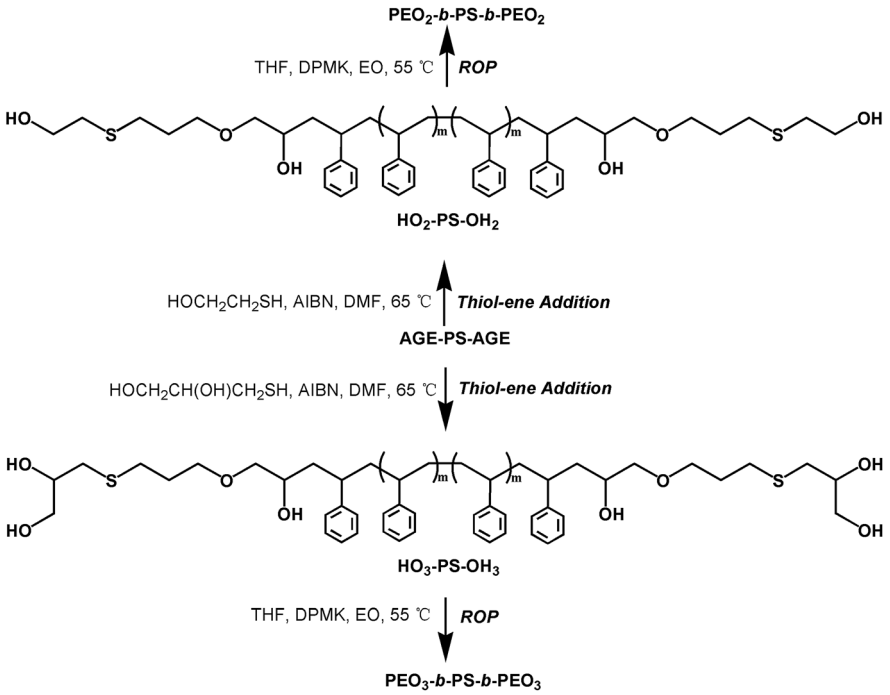

Scheme 3 The synthetic procedure of copolymers PEO_2-*b*-PS-*b*-PEO_2, PEO_3-*b*-PS-*b*-PEO_3 and their precursor.

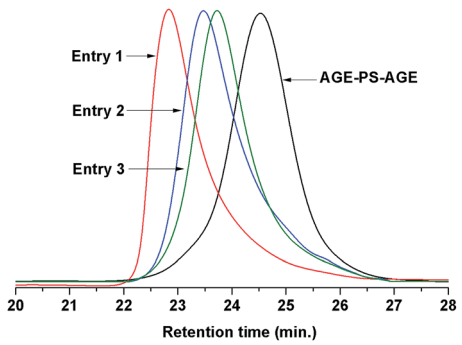

Fig. 1 GPC traces of polymers AGE-PS-AGE (M_n = 3700 g mol^{-1}, PDI = 1.10), PEO-*b*-PS-*b*-PEO (Entry 1, M_n = 11 500 g mol^{-1}, PDI = 1.11), PEO_2-*b*-PS-*b*-PEO_2 (Entry 2, M_n = 7700 g mol^{-1}, PDI = 1.16), and PEO_3-*b*-PS-*b*-PEO_3 (Entry 3, M_n = 7600 g mol^{-1}, PDI = 1.10).

elsewhere.[15b] All other reagents and solvents were purchased from SCR and used as received.

Characterization

Gel permeation chromatography (GPC) of the polymers was performed in THF at 35 °C with an elution rate of 1.0 mL min^{-1} on an Agilent 1100 equipped with a G1310A pump, a G1362A refractive index detector, and a G1314A variable wavelength detector. One 5 μm LP gel column (500 E, molecular range 500–2 × 10^4 g mol^{-1}) and two 5 μm LP gel mixed bed columns (molecular range 200–3 × 10^6 g mol^{-1}) were calibrated by PS standards. ^{1}H NMR spectra were recorded on a Bruker (400 MHz) spectrometer in $CDCl_3$ with tetramethylsilane (TMS) as the internal standard. The MALDI-TOF MS measurement was performed using a Perspective Biosystem Voyager-DE STR MALDI-TOF (matrix-assisted laser desorption/ionization time-of-flight) mass spectrometer (PE Applied Biosystems, Framingham, MA). The accelerating voltage, grid voltage and delay time were optimized for each sample and all the spectra were recorded in reflectron mode. Matrix solution of dithranol (20 mg mL^{-1}), end-functionalized polymer (10 mg mL^{-1}) and cationizing salt of silver trifluoroacetate (10 mg mL^{-1}) in THF were mixed in the ratio of matrix : cationizing salt : polymer = 10 : 1 : 2, and 0.8 μL of mixed solution was deposited on the sample holder (well-plate). Differential scanning calorimetry

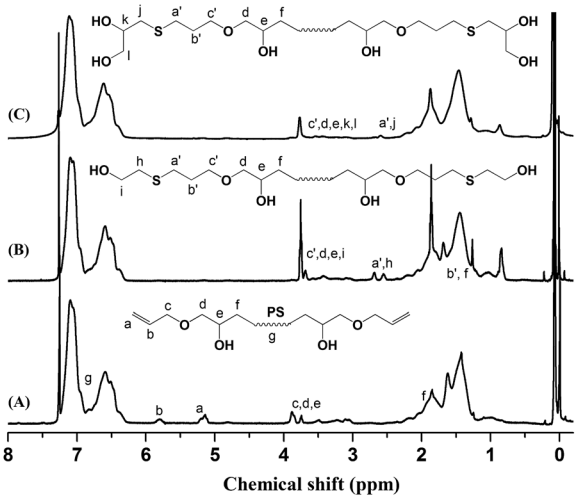

Fig. 2 ^{1}H NMR spectra of (A) AGE-PS-AGE, (B) ME-PS-ME, and (C) MP-PS-MP (in $CDCl_3$).

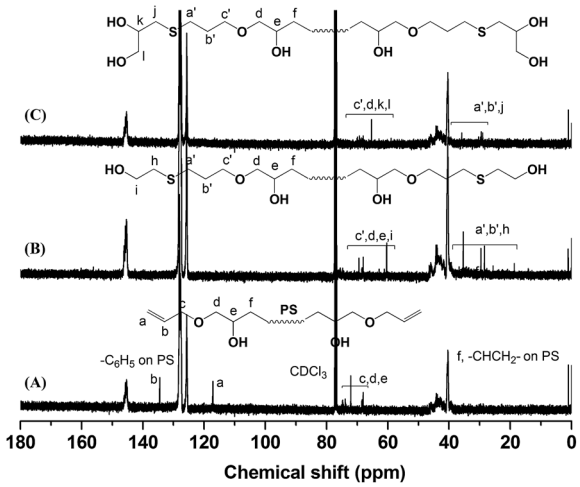

Fig. 3 ^{13}C NMR spectra of (A) AGE-PS-AGE, (B) ME-PS-ME, and (C) MP-PS-MP (in $CDCl_3$).

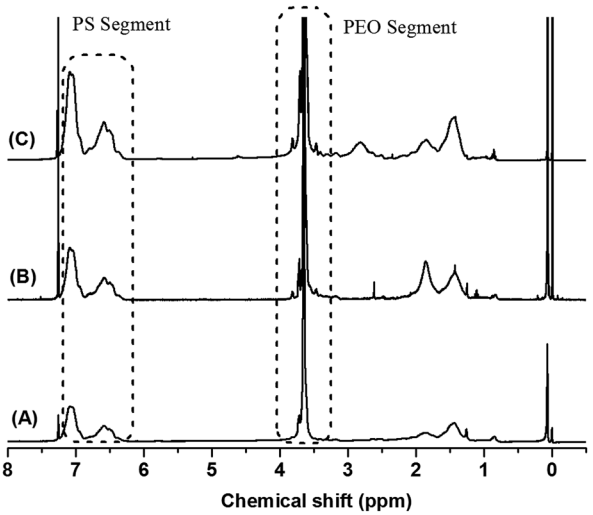

Fig. 5 ^1H NMR spectra of PEO_3-*b*-PS-*b*-PEO_3 with the same PS segment but different length of PEO segments: (A) Entry 3, (B) Entry 4, and (C) Entry 5 (in $CDCl_3$).

(DSC) was carried on a DSC Q2000 thermal analysis system (Shimadzu, Japan). The samples were first heated from −80 °C to 150 °C at a heating rate of 10 °C min^{-1} under nitrogen atmosphere, followed by cooling to −80 °C at 10 °C min^{-1} after stopping at 150 °C for 5 min, and finally heating to 150 °C at 10 °C min^{-1} after stopping at −80 °C for 5 min. X-ray diffraction (XRD) measurements were carried out using an XPert PRO (PANalytical) with Cu Kα (1.541 Å) radiation (40 kV, 40 mA). Samples were exposed at a scanning rate of $2\theta = 5$ °C min^{-1} between 2θ values of 10° to 40°. Crystal growth was observed under a polarized optical microscope (POM, Leica, DM 2500P). The concentration of copolymer was 5 mg mL^{-1}, dichloromethane (CH_2Cl_2) was used as solvent, and all the measurements were carried out at 25 °C.

Synthesis of polystyrene functionalized with allyl glycidyl ether (AGE-PS-AGE)

The sample of AGE-PS-AGE was obtained by the LAP of St monomers initiated by lithium naphthalenide followed by the end-capping reaction with AGE agent (Scheme 2). The lithium naphthalenide initiator was first synthesized from naphthalene and lithium according to our previous work,[41] and the concentration of 0.71 mol L^{-1} was found by titration using hydrochloric acid (0.1 mol L^{-1}). Typically, cyclohexane (700 mL), styrene (50.0 mL, 0.43 mol), and THF (6.0 mL) were sequentially introduced into a 1 L ampule. In order to consume the remaining impurities in the ampule, *n*-Bu^-Li^+ solution was firstly added dropwise until the mixture turned yellowish, and then the needed lithium naphthalenide solution (35.0 mL, 24.9 mmol) was added rapidly. After the reaction was stirred at 25 °C for 50 min, the AGE agent (10.0 mL, 84.5 mmol) dissolved in THF (20 mL) was added, and the red solution changed into faint yellow immediately. The solution was stirred for another 2.0 h at 25 °C and terminated with acidic methanol (0.1 HCl in CH_3OH). After all the solvents were evaporated, the product was recovered by precipitation three times in methanol and dried under vacuum at 45 °C. Yield: 44.6 g (98%). ^1H NMR ($CDCl_3$) δ (ppm):

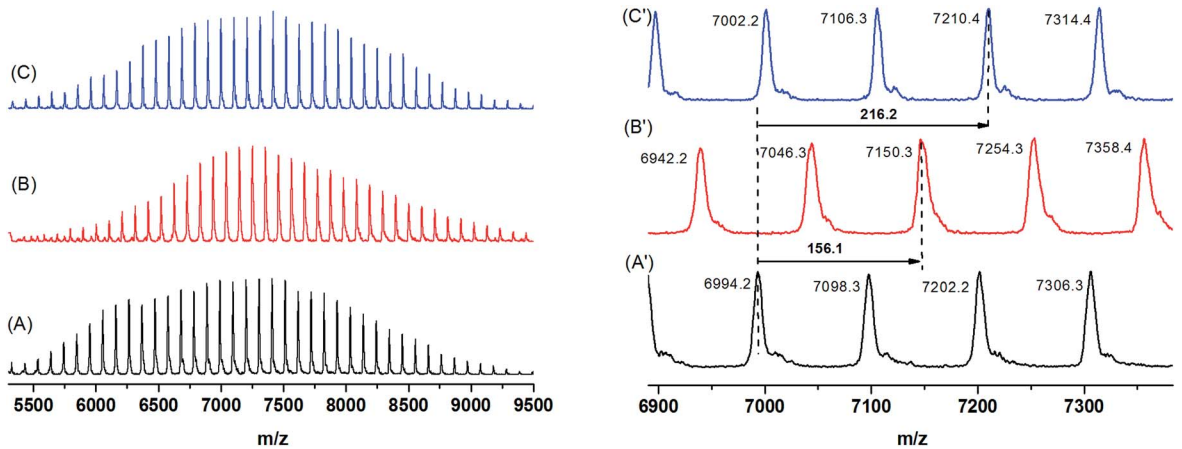

Fig. 4 The MALDI-TOF MS of (A and A′) AGE-PS-AGE ($M_{n,\ GPC}$ = 7500 g mol^{-1}), (B and B′) ME-PS-ME, and (C and C′) MP-PS-MP.

Table 1 Data for dumbbell shaped copolymers of PEO_x-*b*-PS-*b*-PEO_x and their precursors

Entry	Samples	$M_{n,\ GPC}$[a] (g mol^{-1})	PDI[a]	$M_{n,\ NMR}$[b] (g mol^{-1})	DP_{PS}[c]	DP_{PEO}[d]	Percentage of PEO segment[e] (%)
	AGE-PS-AGE	3700	1.14	2500[f]	23		
1	PEO-PS-PEO	11 500	1.11	11 000	23	193	78.02
2	PEO_2-PS-PEO_2	7700	1.16	10 400	23	180	76.80
3	PEO_3-PS-PEO_3	7600	1.10	9100	23	150	73.40
4	PEO_3-PS-PEO_3	7400	1.13	8100	23	127	68.99
5	PEO_3-PS-PEO_3	7000	1.09	6000	23	80	59.54
	AGE-PS-AGE	7900	1.14	7500[f]	71		
6	PEO-PS-PEO	14 700	1.17	22 000	71	330	66.29
7	PEO-PS-PEO	9100	1.09	13 300	71	132	44.03
8	PEO_2-PS-PEO_2	7900	1.11	9400	71	43	20.40
9	PEO_3-PS-PEO_3	9800	1.14	11 700	71	95	36.15

[a] Determined by GPC with THF as solvent using PS standards. [b] The molecular weights of copolymers were calculated according to ^{1}H NMR using formula (1). [c] The degree of polymerization (DP_{PS}) was calculated according to the formula: $DP_{PS} = M_{n,\ MALDI\text{-}TOF\ MS,\ PS}/104$. [d] The degree of polymerization (DP_{PEO}) was calculated according to the formula: $DP_{PEO} = (M_{n,\ NMR,\ (PEO_x\text{-}b\text{-}PS\text{-}b\text{-}PEO_x)} - M_{n,\ MALDI\text{-}TOF\ MS,\ PS})/44$. [e] The percentage of PEO segment (%) was calculated according to the formula: $\%_{PEO} = D_{PEO_x}44/M_{n,\ NMR,\ (PEO_x\text{-}b\text{-}PS\text{-}b\text{-}PEO_x)}$. [f] Determined by MALDI-TOF MS measurement.

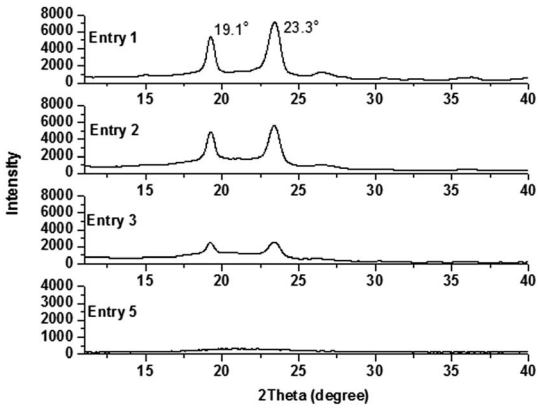

Fig. 6 X-ray diffraction patterns for PEO-*b*-PS-*b*-PEO (Entry 1), PEO_2-*b*-PS-*b*-PEO_2 (Entry 2), and PEO_3-*b*-PS-*b*-PEO_3 (Entry 3 and Entry 5).

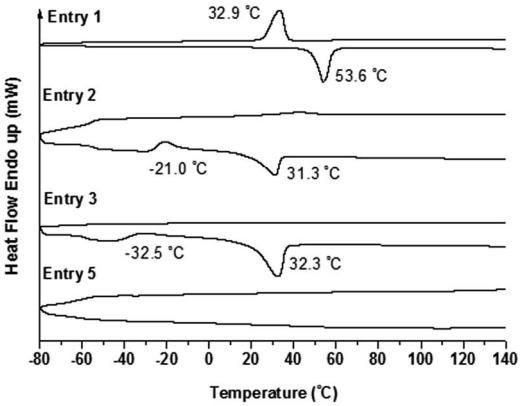

Fig. 8 DSC traces of copolymer PEO-*b*-PS-*b*-PEO (Entry 1), PEO_2-*b*-PS-*b*-PEO_2 (Entry 1), and PEO_3-*b*-PS-*b*-PEO_3 (Entry 3 and Entry 5).

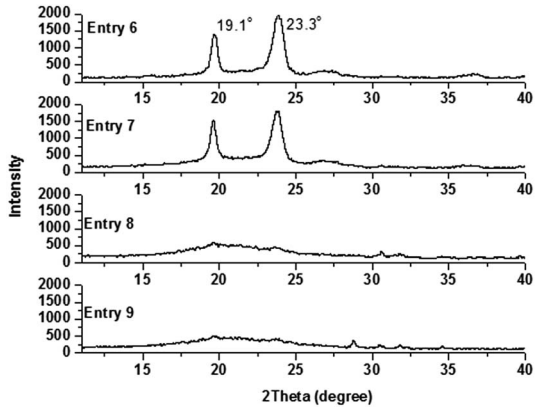

Fig. 7 X-ray diffraction patterns for PEO-*b*-PS-*b*-PEO (Entry 6 and Entry 7), PEO_2-*b*-PS-*b*-PEO_2 (Entry 8), and PEO_3-*b*-PS-*b*-PEO_3 (Entry 9).

1.11–2.25 ($C_6H_5CHCH_2$–, –CH_2CHOH), 3.50–4.00 (–CH(OH), –CH_2OCH_2–), 5.08–5.25 (CH_2=CH–), 5.74–5.86 (CH_2=CH–), 6.28–7.22 (–C_6H_5–). $M_{n,\ GPC}$ = 3700 g mol^{-1}, PDI = 1.10, $M_{MALDI\text{-}TOF\ MS}$ = 2500 g mol^{-1}.

Synthesis of polystyrene functionalized with 2-mercaptoethanol and 3-mercapto-1,2-propanediol (ME-PS-ME and MP-PS-MP)

The functionalized precursors of ME-PS-ME and MP-PS-MP were achieved by the thiol-ene addition reaction (Scheme 3).

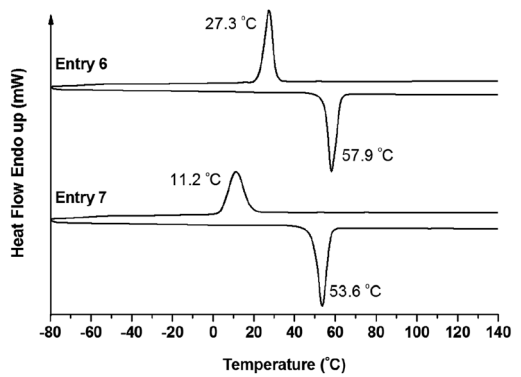

Fig. 9 DSC traces of copolymer PEO-*b*-PS-*b*-PEO (Entry 6 and Entry 7).

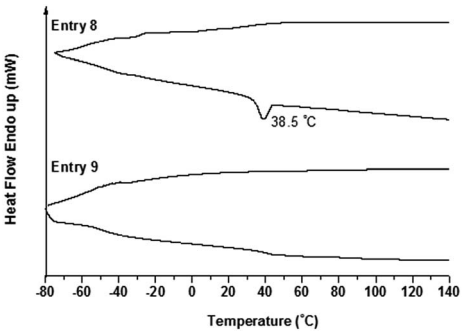

Fig. 10 DSC traces of copolymers PEO_2-*b*-PS-*b*-PEO_2 (Entry 8), and PEO_3-*b*-PS-*b*-PEO_3 (Entry 9).

Typically, AGE-PS-AGE (10.0 g, 2.7 mmol), AIBN (1.64 g, 10 mmol) and ME (2.5 mL, 25 mmol) were dissolved in 80.0 mL dimethylformamide (DMF) in a 200 mL ampoule. After the reaction system was degassed by three cycles of freeze–pump–thaw, the ampoule was filled with nitrogen and then maintained at 65 °C for 24 h. Finally, the solvents were removed by reduced distillation, and the ME-PS-ME was obtained by precipitation three times in methanol and dried under vacuum at 45 °C. Yield: 9.8 g (96%). ^{1}H NMR ($CDCl_3$) δ (ppm): 1.20–2.10 ($C_6H_5CHCH_2$–, –$CH_2CH_2CH_2$–, –CH_2CHOH), 2.54–2.69 (–CH_2SCH_2–), 2.98–3.95 (–CH_2(OH), –CH_2OCH_2–, –CH_2CHOH), 6.33–7.25 (–C_6H_5–).

Similarly, the synthetic procedure of MP-PS-MP was the same as that of ME-PS-ME, except that the ME agent was replaced by the MP agent. ^{1}H NMR ($CDCl_3$) δ (ppm): 1.16–2.20 ($C_6H_5CHCH_2$–), 2.52–2.72 (–CH_2SCH_2–), 2.92–3.95 (–CH_2(OH), –CHOH, –CH_2OCH_2–), 6.28–7.22 (–C_6H_5–).

Synthesis of dumbbell shaped copolymer PEO_x-*b*-PS-*b*-PEO_x ($x = 1, 2, 3$)

The copolymer PEO-*b*-PS-*b*-PEO was obtained by the ROP of EO monomers using AGE-PS-AGE as macro-initiator (Scheme 3). Typically, dry AGE-PS-AGE (6.0 g, 1.6 mmol) was dissolved in 200 mL THF and charged into a 500 mL dry ampoule, and the calculated DPMK solution (4.0 mL, 3.0 mmol) was added dropwise by a syringe under magnetic stirring. Then the ampoule was placed into an ice bath and cold EO (15.0 mL, 0.29 mol) monomers were added quickly, and the solution was heated to 55 °C and stirred for 96 h. The solution was finally terminated by acid methanol (0.1 HCl in CH_3OH) and the solvents were evaporated. Subsequently, the copolymers PEO-*b*-PS-*b*-PEO were precipitated in cold petroleum ether (30–60 °C) slowly three times and dried under vacuum at 45 °C for 12 h to a constant weight. Yield: 9.8 g (96%). ^{1}H NMR ($CDCl_3$) δ (ppm): 3.59–3.70 (–CH_2CH_2O–), 6.28–7.22 (–C_6H_5–). $M_{n,\ GPC} = 11\ 500$ g mol^{-1}, PDI = 1.10, $M_{n,\ NMR} = 11\ 000$ g mol^{-1}.

Similarly, the copolymers PEO_2-*b*-PS-*b*-PEO_2 and PEO_3-*b*-PS-*b*-PEO_3 were also prepared by the ROP of EO monomers from macro-initiators of ME-PS-ME and MP-PS-MP, respectively (Scheme 3). By changing the feed molar ratio of macro-initiators to EO monomers, copolymers with different compositions could be realized.

Results and discussion

Synthesis and characterization of amphiphilic dumbbell shaped copolymers PEO_x-*b*-PS-*b*-PEO_x

The key precursor AGE-PS-AGE with one active hydroxyl group and one allyl group at each end was designed and synthesized by LAP mechanism and the subsequent end-capping reaction with an oxirane ring on AGE agent. This versatile precursor could be further selectively modified by thiol-ene addition reaction. Subsequently, by combination of ROP mechanism, the target copolymers PEO_x-*b*-PS-*b*-PEO_x ($x = 1, 2, 3$) with different numbers of arms and compositions could be conveniently realized.

Firstly, the difunctional living $^+$Li-PS$^-$Li$^+$ species grown from lithium naphthalenide were carefully end-capped with AGE agent. According to previous work by Quirk,[42] they synthesized several functionalized polymers with high efficiencies (usually >95.0%) by capping the living species with an oxirane ring on a substituted epoxy, such as 1-butene oxide, 3,4-epoxy-1-butene, styrene oxide, and so on. Also, in our work on the functionalization of PS$^-$Li$^+$ with 1-ethoxyethyl glycidyl ether (EEGE),[43] the capping reaction was again realized with a quantitative efficiency. All these references gave the result that the capping reaction between the living species and oxirane ring was rather efficient, quantitative and accompanied by almost no side reactions, which was mainly due to the high aggregation degree of lithium alkoxides and their disability to initiate the further polymerization of the oxirane ring. In this work, because of the inertness of allyl group, the living species just attacked the oxirane ring on AGE, and a new hydroxyl group was simultaneously generated (Scheme 2). Once the AGE agent was added into the red system of the $^+$Li-PS$^-$Li$^+$ solution, one could observe that the color of the system changed into light yellow immediately, which meant that alkoxide (–O$^-$Li$^+$) species was actually formed. In order to ensure the high efficiency of the end-capping reaction, excess AGE agent (nine-fold) was fed. The successful LAP of St monomers was evidenced by the monomodal peak and symmetrical GPC curve with a narrow molecular weight distribution (PDI = 1.10) (Fig. 1). Also, the ^{1}H NMR (Fig. 2A) and ^{13}C NMR (Fig. 3A) spectra of the synthesized AGE-PS-AGE were monitored. In Fig. 2A, except for the characteristic resonance signals of aromatic protons (–C_6H_5–) on the PS chain seen at 6.28–7.22 ppm, the resonance signals appearing at 5.16 ppm (CH_2=CH–) and 5.78 ppm (CH_2=CH–) confirmed the successful introduction of the allyl group onto PS. Also, signals ascribed to methane and methylene protons (–CH(OH)CH_2-OCH_2CH=CH_2) were observed at 3.50–4.00 ppm. In Fig. 3A, the characteristic resonance signals of carbon atoms (–C_6H_5–) were seen at 124–130 ppm, and the characteristic resonance signals of carbon atoms (CH_2=CH–) and (CH_2=CH–) were seen at 117 ppm and 134 ppm, respectively. Thus, the NMR results actually proved the smooth coupling reaction of AGE agent with living $^+$Li-PS$^-$Li$^+$ species and the successful introduction of the allyl group onto PS. Furthermore, the functionalized AGE-PS-AGE with defined structure was again analyzed by MALDI-TOF MS (Fig. 4). As shown in Fig. 4A, a series of mono-peaks were

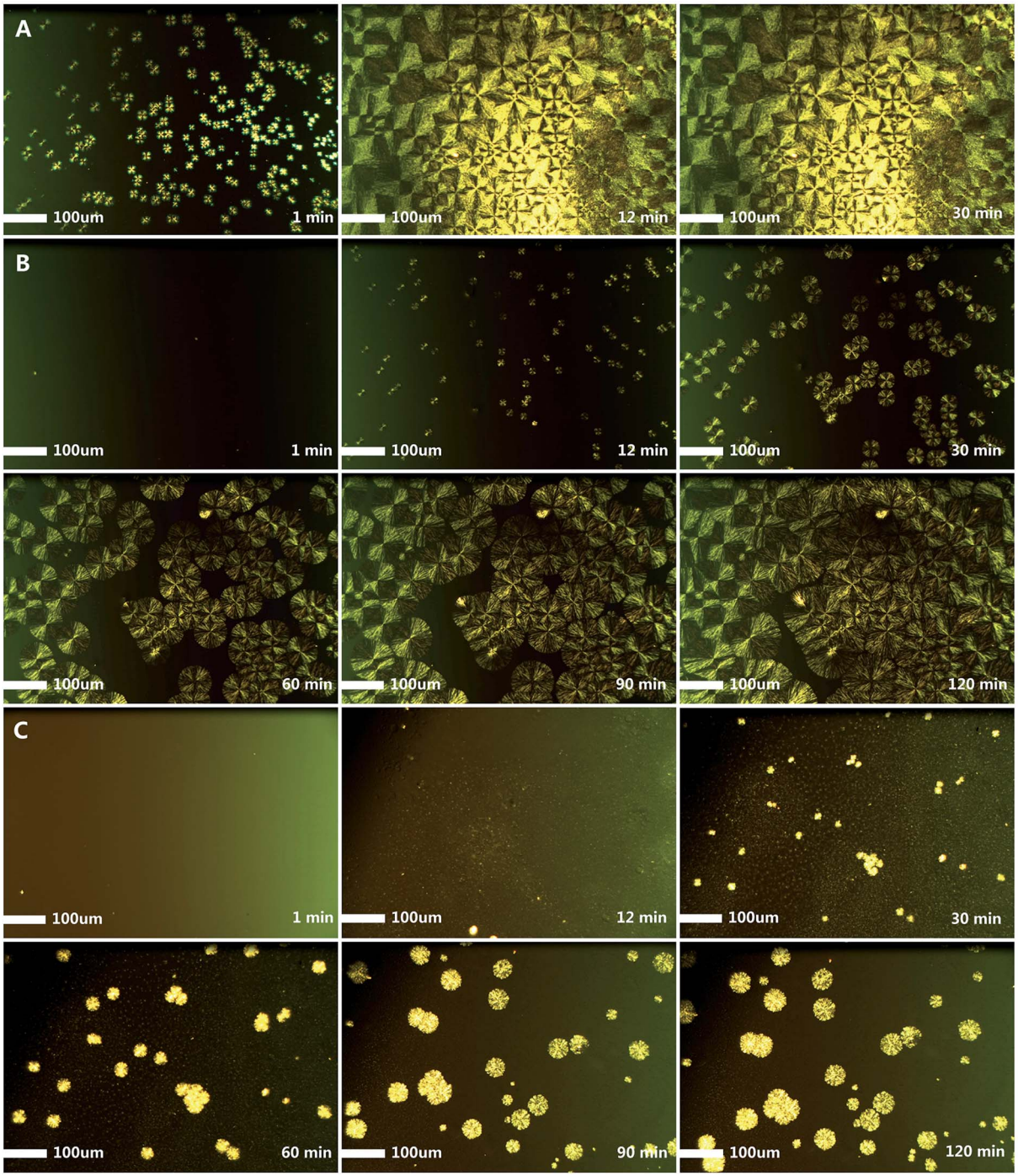

Fig. 11 Optical microscopy images of copolymers (scale bar = 100 μm): (A) PEO-*b*-PS-*b*-PEO (Entry 1), (B) PEO_2-*b*-PS-*b*-PEO_2 (Entry 2), and (C) PEO_3-*b*-PS-*b*-PEO_3 (Entry 3).

observed for AGE-PS-AGE. When the mass spectrum was expanded (Fig. 4A′), the peak at m/z = 6994.2 (a monoisotopic mass peak) was attributed to the functionalized AGE-PS-AGE [$C_6H_{10}O_2$–$(C_8H_8)_{64}$–$C_6H_{10}O_2 \cdot Ag^+$ = 6994.2, cal. 6994.39], and the m/z spacing of 104.1 between adjacent peaks was the mass of St monomeric unit. The absence of any minor peak series confirmed that the capping reaction at both $^+$Li-PS$^-$Li$^+$ ends was rather successful and a high efficiency was achieved. According to the integral areas at 5.16 ppm (C***H***$_2$=CH–), 5.78 ppm (CH$_2$=C***H***–), 6.28–7.22 ppm and the absolute molecular weight of AGE-PS-AGE obtained by MALDI-TOF MS, the capping efficiency of the AGE agent to $^+$Li-PS$^-$Li$^+$ was calculated as 98.5%.

Subsequently, by efficient thiol-ene addition reaction, one allyl group could be transformed into one or two hydroxyl groups. Using DMF as solvent and AIBN as catalyst, the ME-PS-ME with two hydroxyl groups at each end was obtained by the

reaction between 2-mercaptoethanol and the above AGE-PS-AGE (Scheme 3). From the ^{1}H NMR spectrum of ME-PS-ME (Fig. 2B), the disappearance of the resonance signals at 5.16 ppm (CH_2=CH–) and 5.78 ppm (CH_2=C**H**–) confirmed that the allyl groups were completely consumed. Also, the appearance of signals at 2.54 ppm and 2.69 ppm assigned to the methylene protons connected to sulfur atom (–C**H**$_2$–S–C**H**$_2$–) further confirmed the successful introduction of 2-mercaptoethanol. Similarly, the MP-PS-MP was obtained by the thiol-ene addition reaction between AGE-PS-AGE and 3-mercapto-1,2-propanediol. The complete disappearance of resonance signals at 5.16 ppm and 5.78 ppm assigned to the allyl group confirmed that an almost 100% efficiency of thiol-ene addition reaction was realized. From the ^{13}C NMR spectra of ME-PS-ME (Fig. 3B) and MP-PS-MP (Fig. 3C), the complete disappearance of characteristic signals ascribed to carbon atoms at 117 ppm (**C**H$_2$=CH–) and 134 ppm (CH_2=**C**H–) and the new occurrence of signals ascribed to the carbon atoms on the ME or MP groups also gave the same information that the allyl groups at the PS end were completely transformed into the corresponding target groups. Again, the efficient transformations from AGE-PS-AGE to ME-PS-ME and MP-PS-MP were confirmed by MALDI-TOF MS measurement (Fig. 4). As shown in Fig. 4, an increase of 156.1 *m*/*z* from peak [$C_6H_{10}O_2$–$(C_8H_8)_{64}$–$C_6H_{10}O_2$·Ag^+ = 6994.2, cal. 6994.39] to peak [C_2H_6OS–$C_6H_{10}O_2$–$(C_8H_8)_{64}$–$C_6H_{10}O_2$–C_2H_6OS·Ag^+ = 7150.3] was attributed to the mass of two introduced 2-mercaptoethanol units, and the increase of 216.2 *m*/*z* from peak [$C_6H_{10}O_2$–$(C_8H_8)_{64}$–$C_6H_{10}O_2$·Ag^+ = 6994.2, cal. 6994.39] to peak [$C_3H_8O_2S$–$C_6H_{10}O_2$–$(C_8H_8)_{64}$–$C_6H_{10}O_2$–$C_3H_8O_2S$·Ag^+ = 7210.4] was attributed to the mass of two introduced 3-mercapto-1,2-propanediol units. Thus, the perfectly coincident results from MALDI-TOF MS and NMR gave the information that the macro-initiators of ME-PS-ME and MP-PS-MP were successfully synthesized.

Finally, the target copolymers PEO$_x$-*b*-PS-*b*-PEO$_x$ were obtained by the ROP of EO monomers using the above AGE-PS-AGE, ME-PS-ME and MP-PS-MP as macro-initiators and DPMK as deprotonation agent (Scheme 3). Typically, because of the rapid exchange ratio (which was faster than the propagation ratio) between living species –O$^-$K$^+$ and the dormant –OH, the ROP mechanism was endowed with a living character. According to the literature,[44] primary and secondary hydroxyls could give the uniform growth of PEO chains under certain polymerization conditions. Using the similar polymerization system in this contribution, all the hydroxyl groups had the ability to initiate the polymerization of EO monomers, and the designed architecture of PEO$_x$-*b*-PS-*b*-PEO$_x$ with defined numbers of arms could be obtained. From Fig. 1, it could be observed that the GPC traces of the obtained PEO-*b*-PS-*b*-PEO, PEO$_2$-*b*-PS-*b*-PEO$_2$ and PEO$_3$-*b*-PS-*b*-PEO$_3$ all have monomodal peaks and low PDIs, which also gave the conclusion that the ROP mechanism proceeded smoothly. However, an asymmetrical GPC trace with a tail at longer elution time was always detected due to the strong adsorption of the PEO segment with the column in THF solvent (which was not a good solvent for the PEO segment), rather than the existence of PS homopolymers, and a similar phenomenon was also reported in our previous work[43] and other's work.[45] In order to further confirm this consumption, the copolymers were verified by the TLC method using THF as developing agent. The absence of any PS signal in the front edge under 254 nm on the UV detector confirmed that there was actually not any PS homopolymer existing in the copolymers. The composition of the copolymers was further studied by the ^{1}H MNR spectrum. In order to avoid the formation of micelles in selective solvent,[2a,45] the ^{1}H NMR measurement of the copolymers was carried out in $CDCl_3$ solvent, which was a good solvent for both the PEO and PS segments.[46] As shown in Fig. 5, the characteristic resonance signal of aromatic protons (–C$_6$**H**$_5$–) on the PS segment at 6.28–7.22 ppm and that of methylene protons (–C**H**$_2$C**H**$_2$O–) on the PEO segment at 3.05–3.70 ppm were discriminated well. On the other hand, the molecular weight of PEO$_x$-*b*-PS-*b*-PEO$_x$ determined by GPC measurement using THF as an eluent was unreliable because THF was not a good solvent for the PEO segment and the PEO$_x$-*b*-PS-*b*-PEO$_x$ might aggregate into micellar structures by self-association in THF; this phenomenon was also reported in ref. 2*a* and 47 and our previous work.[43] Alternatively, according to the above ^{1}H MNR spectrum and the already known absolute molecular weight of the AGE-PS-AGE precursor, the accurate molecular weight of the copolymers could be derived from the formula:

$$M_{n,\,NMR} = \frac{A_{PEO}/4}{A_{PS}/5} \times \frac{M_{n,\,MALDI\text{-}TOF\ MS,\,PS}}{104} \times 44 + M_{n,\,MALDI\text{-}TOF\ MS,\,PS} + 2 \times R \quad (1)$$

Here, A_{PEO} and A_{PS} represent the integral areas of the resonance signals of aromatic protons (–C$_6$**H**$_5$–) at 6.28–7.22 ppm and methylene protons (–C**H**$_2$C**H**$_2$O–) at 3.59–3.70 ppm, respectively. $M_{n,\,MALDI\text{-}TOF\ MS,\,PS}$ is the absolute molecular weight of the AGE-PS-AGE precursor obtained from MALDI-TOF MS measurement. The values of 104 and 44 are the molecular weights of the St and EO monomeric units, respectively. *R* is equal to 0 (for PEO-*b*-PS-*b*-PEO), 78 (for PEO$_2$-*b*-PS-*b*-PEO$_2$) or 108 (for PEO$_3$-*b*-PS-*b*-PEO$_3$), and the values of 78 and 108 correspond to the molecular weights of the introduced ME and MP residues, respectively.

Interestingly, comparing the molecular weights of the copolymers obtained from GPC with that from the NMR measurement, one can also discern that the apparent molecular weights from the GPC measurement had low linear dependence on their absolute molecular weights from NMR measurement. For example, PEO-*b*-PS-*b*-PEO in Entry 1 and PEO$_2$-*b*-PS-*b*-PEO$_2$ in Entry 2 had a difference of 600 g mol^{-1} in their absolute molecular weights from NMR measurement, however, there was a difference of 3800 g mol^{-1} from their GPC measurement. Alternatively, the samples in Entry 2, Entry 3, Entry 4 and Entry 5 had very similar apparent molecular weights from GPC measurement, however, there was much difference between their absolute molecular weights. These phenomena could be attributed to the varied length of the PEO segments and the increasing branching of copolymers from PEO-*b*-PS-*b*-PEO to PEO$_2$-*b*-PS-*b*-PEO$_2$ and PEO$_3$-*b*-PS-*b*-PEO$_3$. Also, these phenomena might give the information that the

topologies of copolymers actually induced some special properties of the copolymers, and the crystallization behavior of these synthesized copolymers will be discussed in the following section.

The crystallization behavior of copolymers PEO_x-*b*-PS-*b*-PEO_x

Typically, the PS is an amorphous segment, while the PEO is a crystalline segment.[48] As shown in Table 1, PS and PEO segments with different lengths were designed and synthesized by the versatile LAP and ROP mechanisms. As an important target, the crystallization behaviors of these synthesized copolymers were investigated and compared in this contribution.

The crystallization behavior of PEO_x-*b*-PS-*b*-PEO_x was firstly studied by XRD measurement. All the samples were measured at room temperature without annealing. Typically, the linear PEO showed two intense diffraction peaks at 19.1° and 23.3°.[49] As shown in Fig. 6, with a similar percentage of the PEO segment but varied numbers of side PEO arms, the intensity of the diffraction peaks for the PEO crystallite decreased from the copolymer PEO-*b*-PS-*b*-PEO (Entry 1) to PEO_2-*b*-PS-*b*-PEO_2 (Entry 2) and PEO_3-*b*-PS-*b*-PEO_3 (Entry 3). For these three samples with the similar percentages of the PEO segment, the lengths of the PEO arms were shortened with the increase of the number of side arms, and correspondingly, the shorter PEO segment and the increased terminal PEO ends severely interrupted the crystallization abilities of the copolymers.

Alternatively, when the numbers of PEO arms were fixed but their percentages were varied, the crystallization behavior of the copolymers led to another result. Comparing the XRD trace for Entry 3 with that for Entry 5, no diffraction signals could be observed in the XRD trace for the latter when the PEO content was merely decreased to 59.54%. However, comparing the XRD trace for Entry 6 with that for Entry 7, strong signals could still be discriminated at 19.1° and 23.3° even though the PEO content was decreased to 44.03% for Entry 7 (Fig. 7). These results preliminarily gave the conclusion that the degree of branching has more effect on the crystallization behavior than the percentage of the PEO segment.

Furthermore, the crystallization behavior of the copolymers was verified by DSC measurement. The crystallization temperature (T_c) was obtained from the cooling run, and the melting temperature (T_m) was obtained from the second heating run. Usually, for the linear PEO homopolymer with a molecular weight of about $M_n = 5000$ g mol^{-1}, T_m and T_c were observed at 63.9 °C and 43.9 °C, respectively.[50] As shown in Fig. 8, for the sample of PEO-*b*-PS-*b*-PEO (Entry 1), T_c and T_m were clearly discriminated at 32.9 °C and 53.6 °C, respectively, which were both lower than for the PEO homopolymer. However, for the sample of PEO_2-*b*-PS-*b*-PEO_2 (Entry 2), which had a similar percentage of the PEO segment but a different number of side PEO arms compared to the sample in Entry 1, except for a decreased T_m peak at 31.3 °C and a T_c peak at −21.0 °C observed in the heating curve, there was almost not any T_c detected in the cooling run. We concluded that, because of the increased complexity of the architecture of PEO_2-*b*-PS-*b*-PEO_2 in Entry 2, the PEO segment could not be arranged into a crystalline form in the cooling program, and the insufficient crystallization of the PEO segment was maintained in the sample. Alternatively, in the following heating program, some of the PEO segment in the amorphous phase might again be folded into a crystalline form under certain temperatures by a thermal crystallization procedure. This phenomenon has also been reported in ref. 51. Similarly, the sample of PEO_3-*b*-PS-*b*-PEO_3 (Entry 3) also gave a T_c at −32.5 °C corresponding to thermal crystallization and a typical T_m at 32.3 °C in the heating curve, and there was also not any T_c observed in the cooling curve.

Again, for the samples with the same number of PEO arms but varied percentage of the PEO segment, the DSC results of the PEO_3-*b*-PS-*b*-PEO_3 series also gave a different tendency to those of the PEO-*b*-PS-*b*-PEO series. For example, comparing the DSC curve for Entry 3 with that for Entry 5 (Fig. 8), no peaks could be discriminated in the DSC curve for the latter, Entry 5, because of the decreased percentage of the PEO segment (59.54%). However, comparing the DSC curve for Entry 6 with that for Entry 7 (Fig. 9), both samples gave DSC curves with defined T_m and T_c peaks (even though the percentage of the PEO segment in the latter, Entry 7, decreased to 44.03%) because of the linear architecture of PEO-*b*-PS-*b*-PEO.

From Fig. 10, for the DSC curves of Entry 8 and Entry 9, there was almost no obvious signal for the crystallization behavior (such as T_m and T_c peaks) of the samples, except that there was a weak T_m peak at 38.5 °C, which was rather consistent with the results from their XRD measurements (Fig. 7). This might be attributed to the largely lowered PEO content or increased number of side arms, as well as the increased length of the PS segment. On the other hand, it was worth noting that even with the increased length of PS segment (7500 g mol^{-1}) for samples in Entry 8 and Entry 9, no trace of the glass transition temperature (T_g) for the PS segment could be discriminated.

Thus, the DSC results again gave the information that the degree of branching would have a greater effect on the crystallization behavior of the copolymers than the percentage of individual segments.

Finally, the crystallization behavior was also investigated by POM measurement (Fig. 11). From the POM micrograph of PEO-*b*-PS-*b*-PEO (Entry 1), we clearly observed that the big spherulites of the PEO segments could be formed in 30 minutes. With the increase of the number of PEO arms, the crystallization behavior was significantly affected. Obviously, from the sample of PEO-*b*-PS-*b*-PEO (Entry 1) to PEO_2-*b*-PS-*b*-PEO_2 (Entry 2) and PEO_3-*b*-PS-*b*-PEO_3 (Entry 3), a longer crystallization time was needed and only smaller spherulites could be observed.

All the above results indicated that the degree of branching and compositions actually exerted some important effects on the crystallization behaviors of synthesized dumbbell shaped copolymers PEO_x-*b*-PS-*b*-PEO_x. The existence of a PS segment largely interrupted the crystallization behavior of the PEO segment, and the existence of a crystalline PEO segment largely restricted the mobility of the PS segment and affected its T_g. Comprehensively, the degree of branching derived from various complicated topologies might make the primary contribution to the crystallization behavior.

Conclusions

A series of well-defined dumbbell shaped copolymers PEO_x-*b*-PS-*b*-PEO_x ($x = 1, 2, 3$) consisting of PEO and PS segments were successfully synthesized by LAP and ROP mechanisms and the efficient thiol-ene addition reaction. This versatile synthetic route might be further explored to synthesize other copolymers with complicated architectures. Also, the crystallization behaviors of the copolymers with similar compositions but different topologies, or conversely, with different compositions but the same topologies, were investigated and compared. The preliminary results confirmed that the topologies of copolymers actually made the primary contribution to the crystallization behavior.

Acknowledgements

We appreciate the financial support of this research by the Natural Science Foundation of China (21274024).

Notes and references

1 (*a*) A. Vazaios, D. J. Lohse and N. Hadjichristidis, *Macromolecules*, 2005, **38**, 5468–5474; (*b*) L. Andruzzi, A. Hexemer, X. F. Li, C. K. Ober, E. J. Kramer, G. Galli, E. Chiellini and D. A. Fischer, *Langmuir*, 2004, **20**, 10498–10506; (*c*) F. J. Xu, Y. Song, Z. P. Cheng, X. L. Zhu, C. X. Zhu, E. T. Kang and K. G. Neoh, *Macromolecules*, 2005, **38**, 6254–6258; (*d*) V. Percec, T. Guliashvili, J. S. Ladislaw, A. Wistrand, A. Stjerndahl, M. J. Sienkowska, M. J. Monteiro and S. Sahoo, *J. Am. Chem. Soc.*, 2006, **128**, 14156–14165; (*e*) H. F. Gao and K. Matyjaszewski, *J. Am. Chem. Soc.*, 2007, **129**, 6633–6639; (*f*) W. H. Binder and R. Sachsenhofer, *Macromol. Rapid Commun.*, 2007, **28**, 15–54.

2 (*a*) H. Zhang and E. Ruckenstein, *Macromolecules*, 2000, **33**, 814–819; (*b*) K. Se, H. Yamazaki, T. Shibamoto, A. Takano and T. Fujimoto, *Macromolecules*, 1997, **30**, 1570–1576.

3 M. Gauthier, L. Tichagwa, J. S. Downey and S. Gao, *Macromolecules*, 1996, **29**, 519–527.

4 C. Lee, H. Lee, W. Lee, T. Chang and J. Roovers, *Macromolecules*, 2000, **33**, 8119–8121.

5 J. Teng and E. R. Zubarev, *J. Am. Chem. Soc.*, 2003, **125**, 11840–11841.

6 N. Hadjichristidis, M. Pitsikalis, S. Pispas and H. Iatrou, *Chem. Rev.*, 2001, **101**, 3747–3792.

7 Y. Yagci and M. A. Tasdelen, *Prog. Polym. Sci.*, 2006, **31**, 1133–1170.

8 S. E. Stiriba, H. Kautz and H. Frey, *J. Am. Chem. Soc.*, 2002, **124**, 9698–9699.

9 R. Djalali, S. Y. Li and M. Schmidt, *Macromolecules*, 2002, **35**, 4282–4288.

10 M. Zhang, M. Drechsler and A. H. E. Muller, *Chem. Mater.*, 2004, **16**, 537–543.

11 L. H. He, J. Huang, Y. M. Chen, X. J. Xu and L. P. Liu, *Macromolecules*, 2005, **38**, 3845–3851.

12 L. Huang, H. Yuan, D. B. Zhang, Z. Zhang, J. Guo and J. M. Ma, *Appl. Surf. Sci.*, 2004, **225**, 39–46.

13 L. M. Wu and Q. C. Zou, *J. Polym. Sci., Part B: Polym. Phys.*, 2007, **45**, 2015–2022.

14 (*a*) Y. Gao and H. L. Liu, *J. Appl. Polym. Sci.*, 2007, **106**, 2718–2723; (*b*) C. Y. Luo, X. Han, Y. Gao, H. L. Liu and Y. Hu, *J. Macromol. Sci., Part B: Phys.*, 2010, **49**, 440–453.

15 (*a*) S. Y. Cheng, Z. S. Xu and J. J. Yuan, *Acta Chim. Sin.*, 2000, **58**, 368–370; (*b*) R. Francis, D. Taton, J. L. Logan, P. Masse, Y. Gnanou and R. S. Duran, *Macromolecules*, 2003, **36**, 8253–8259.

16 (*a*) T. Kimura and Y. Yamauchi, *Langmuir*, 2012, **28**, 12901–12908; (*b*) D. Chandra, M. Bekki, M. Nakamura, S. Sonezaki, T. Ohji, K. Kato and T. Kimura, *J. Mater. Chem.*, 2011, **21**, 5738–5744.

17 (*a*) Y. J. Cheng, M. Wolkenhauer, G. G. Bumbu and J. S. Gutmann, *Macromol. Rapid Commun.*, 2012, **33**, 218–224; (*b*) T. Ghoshal, M. T. Shaw, C. T. Bolger, J. D. Holmes and M. A. Morris, *J. Mater. Chem.*, 2012, **22**, 12083–12089.

18 (*a*) N. V. Salim, T. L. Hanley, L. Waddington, P. G. Hartley and Q. P. Guo, *Macromol. Rapid Commun.*, 2012, **33**, 401–406; (*b*) Y. Zhang, H. Li, Y. Q. Liu and J. Wang, *Chem. Commun.*, 2012, **48**, 8538–8540.

19 (*a*) B. M. Rosen, G. Lligadas, C. Hahn and V. Percec, *J. Polym. Sci., Part A: Polym. Chem.*, 2009, **47**, 3931–3939; (*b*) B. M. Rosen, G. Lligadas, C. Hahn and V. Percec, *J. Polym. Sci., Part A: Polym. Chem.*, 2009, **47**, 3940–3948.

20 (*a*) J. W. Chan, C. E. Hoyle and A. B. Lowe, *J. Am. Chem. Soc.*, 2009, **131**, 5751–5753; (*b*) V. T. Huynh, G. J. Chen, P. D. Souza and M. H. Stenzel, *Biomacromolecules*, 2011, **12**, 1738–1751; (*c*) B. Yu, J. W. Chan, C. E. Hoyle and A. B. Lowe, *J. Polym. Sci., Part A: Polym. Chem.*, 2009, **47**, 3544–3557.

21 (*a*) A. Dondoni, *Angew. Chem., Int. Ed.*, 2008, **47**, 8995–8997; (*b*) C. E. Hoyle and C. N. Bowman, *Angew. Chem., Int. Ed.*, 2010, **49**, 1540–1573.

22 T. Sarbu, K. Y. Lin, J. Ell, D. J. Siegwart, J. Spanswick and K. Matyjaszewski, *Macromolecules*, 2004, **37**, 3120–3127.

23 P. Siemsen, R. C. Livingston and F. Diederich, *Angew. Chem., Int. Ed.*, 2000, **39**, 2632–2657.

24 (*a*) R. Kandre, K. Feldman, H. E. H. Meijer, P. Smith and A. D. Schluter, *Angew. Chem., Int. Ed.*, 2007, **46**, 4956–4959; (*b*) W. G. Huang, L. J. Su and Z. J. Bo, *J. Am. Chem. Soc.*, 2009, **131**, 10348–10349.

25 (*a*) E. C. Hagberg, M. Malkoch, Y. Ling, C. J. Hawker and K. R. Carter, *Nano Lett.*, 2007, **7**, 233–237; (*b*) V. S. Khire, A. W. Harant, A. W. Watkins, K. S. Anseth and C. N. Bowman, *Macromolecules*, 2006, **39**, 5081–5086.

26 (*a*) A. W. Harant, V. S. Khire, M. S. Thibodaux and C. N. Bowman, *Macromolecules*, 2006, **39**, 1461–1466; (*b*) V. S. Khire, T. Y. Lee and C. N. Bowman, *Macromolecules*, 2008, **41**, 7440–7447; (*c*) L. A. Connal, C. R. Kinnane, A. N. Zelikin and F. Caruso, *Chem. Mater.*, 2009, **21**, 576–578.

27 (*a*) V. S. Khire, D. S. W. Benott, K. S. Anseth and C. N. Bowman, *J. Polym. Sci., Part A: Polym. Chem.*, 2006, **44**, 7027–7039; (*b*) A. E. Rydholma, C. N. Bowmana and K. S. Anseth, *Biomaterials*, 2005, **26**, 4495–4506; (*c*) A. Dondoni, *Angew. Chem., Int. Ed.*, 2008, **47**, 8995–8997.

28 M. Sangermano, R. Bongiovanni, G. Malucelli, A. Priola, A. Harden and N. Rehnber, *J. Polym. Sci., Part A: Polym. Chem.*, 2002, **40**, 2583–2590.

29 (*a*) H. Y. Wei, A. F. Senyurt, S. Jonsson and C. E. Hoyle, *J. Polym. Sci., Part A: Polym. Chem.*, 2007, **45**, 822–829; (*b*) J. Shin, S. Nazarenko and C. E. Hoyle, *Macromolecules*, 2008, **41**, 6741–6746; (*c*) L. Kwisnek, S. Nazarenko and C. E. Hoyle, *Macromolecules*, 2009, **42**, 7031–7041.

30 K. L. Killops, L. M. Campos and C. J. Hawker, *J. Am. Chem. Soc.*, 2008, **130**, 5062–5064.

31 C. Rissing and D. Y. Son, *Organometallics*, 2009, **28**, 3167–3172.

32 C. Nilsson, N. Simpson, M. Malkoch, M. Johansson and E. Malmstrom, *J. Polym. Sci., Part A: Polym. Chem.*, 2008, **46**, 1339–1348.

33 L. M. Campos, K. L. Killops, R. Sakai, J. M. J. Paulusse, D. Damiron, E. Drockenmuller, B. W. Messmore and C. J. Hawker, *Macromolecules*, 2008, **41**, 7063–7070.

34 R. L. A. David and J. A. Kornfield, *Macromolecules*, 2008, **41**, 1151–1161.

35 A. Gress, A. Volkel and H. Schlaad, *Macromolecules*, 2007, **40**, 7928–7933.

36 J. S. Parent and S. S. Sengupta, *Macromolecules*, 2005, **38**, 5538–5544.

37 M. Li, P. De, S. R. Gondi and B. S. Sumerlin, *J. Polym. Sci., Part A: Polym. Chem.*, 2008, **46**, 5093–5100.

38 Z. P. Tolstyka, J. T. Kopping and H. D. Maynard, *Macromolecules*, 2008, **41**, 599–606.

39 (*a*) S. Peleshanko, J. Jeong, R. Gunawidjaja and V. V. Tsukruk, *Macromolecules*, 2004, **37**, 6511–6522; (*b*) U. S. Jeng, Y. S. Sun, H. Y. Lee, C. H. Hsu and K. S. Liang, *Macromolecules*, 2004, **37**, 4617–4622.

40 B. Lotz and A. J. Kovacs, *Polym. Prepr. (Am. Chem. Soc., Div. Polym. Chem.)*, 1969, **10**, 820.

41 Y. N. Zhang, G. W. Wang and J. L. Huang, *Macromolecules*, 2010, **4**, 10343–10347.

42 (*a*) R. P. Quirk, Q. Ge, M. A. Arnould and C. Wesdemiotis, *Macromol. Chem. Phys.*, 2001, **202**, 1761–1767; (*b*) R. P. Quirk and G. M. Lizarraga, *Macromolecules*, 1998, **31**, 3424–3430; (*c*) R. P. Quirk, H. Hasgawa, D. L. Gomochak, C. Wesdemiotis and K. Wollyung, *Macromolecules*, 2004, **37**, 7146–7155; (*d*) R. P. Quirk and W. C. Chen, *Macromol. Chem.*, 1982, **183**, 2071–2076; (*e*) R. P. Quirk, D. L. Gomochak, C. Wesdemiotis and M. A. Arnold, *J. Polym. Sci., Part A:Polym. Chem.*, 2003, **41**, 947–957; (*f*) R. P. Quirk and J. J. Ma, *J. Polym. Sci., Part A: Polym. Chem.*, 1988, **26**, 2031–2037; (*g*) R. P. Quirk, D. L. Pickel and H. Hasegawa, *Macromol. Symp.*, 2005, **226**, 69–77.

43 (*a*) G. W. Wang and J. L. Huang, *J. Polym. Sci., Part A: Polym. Chem.*, 2008, **46**, 1136–1150; (*b*) G. W. Wang and J. L. Huang, *Macromol. Rapid Commun.*, 2007, **28**, 298–304.

44 (*a*) X. S. Feng, D. Taton, E. L. Chaikof and Y. Gnanou, *J. Am. Chem. Soc.*, 2005, **127**, 10956–10966; (*b*) X. S. Feng, D. Taton, E. L. Chaikof and Y. Gnanou, *Macromolecules*, 2009, **42**, 7292–7298.

45 (*a*) F. Calderara, Z. Hruska, G. Hurtrez, T. Nugay and G. Riess, *Makromol. Chem.*, 1993, **194**, 1411–1420; (*b*) M. Teodorescu, M. Dimonie, C. Draghici and G. Vasilievici, *Polym. Int.*, 2004, **53**, 1987–1993; (*c*) R. P. Quirk, J. Kim, C. Kausch and M. Chun, *Polym. Int.*, 1996, **39**, 3–10.

46 (*a*) J. L. Hedrick, M. Trollsas, C. J. Hawker, B. Atthoff, H. Claesson, A. Heise, R. D. Miller, D. Mecerreyes, R. Jerome and P. Dubois, *Macromolecules*, 1998, **31**, 8691–8705; (*b*) A. Heise, J. L. Hedrick, M. Trollsas, R. D. Miller and C. W. Frank, *Macromolecules*, 1999, **32**, 231–234.

47 S. Angot, D. Taton and Y. Gnanou, *Macromolecules*, 2000, **33**, 5418–5426.

48 (*a*) A. Boschetti-de-Fierro, A. J. Mueller and V. Abetz, *Macromolecules*, 2007, **40**, 1290–1298; (*b*) N. Lin and A. Dufresne, *Macromolecules*, 2013, **46**, 5570–5583; (*c*) C. He, J. Sun, T. Zhao, Z. Hong, X. Zhuang, X. Chen and X. Jing, *Biomacromolecules*, 2006, **7**, 252–258; (*d*) C. He, J. Sun, J. Ma, X. Chen and X. Jing, *Biomacromolecules*, 2006, **7**, 3482–3489.

49 G. Maglio, G. Nese, M. Nuzzo and R. Palumbo, *Macromol. Rapid Commun.*, 2004, **25**, 1139–1144.

50 C. Y. Liu, K. Lv, B. Huang, C. L. Hou and G. W. Wang, *RSC Adv.*, 2013, **3**, 17945–17953.

51 H. Yu, A. Natansohn, M. A. Singh and I. Torriani, *Macromolecules*, 2001, **34**, 1258–1266.

